



# Binding of $[\text{Cr}(\text{phen})_3]^{3+}$ to transferrin at extracellular and endosomal pHs: Potential application in photodynamic therapy



Pablo F. Garcia <sup>a</sup>, Judith Toneatto <sup>b</sup>, María Jazmín Silvero <sup>a</sup>, Gerardo A. Argüello <sup>a,\*</sup>

<sup>a</sup> Instituto de Investigaciones en Físico Química de Córdoba (INFIQC) CONICET-UNC, Departamento de Físico Química, Facultad de Ciencias Químicas, Universidad Nacional de Córdoba, Córdoba, Argentina

<sup>b</sup> Laboratory of Nuclear Architecture, Instituto de Biología y Medicina Experimental – CONICET, Ciudad Autónoma de Buenos Aires, Argentina

## ARTICLE INFO

### Article history:

Received 17 March 2014

Received in revised form 3 June 2014

Accepted 16 June 2014

Available online 25 June 2014

### Keywords:

Tris(1,10-phenanthroline)chromium(III)

Apotransferrin

Holotransferrin

Binding

Drug delivery

Photodynamic therapy

## ABSTRACT

**Background:** Transferrin is an iron-binding blood plasma glycoprotein that controls the level of free iron in biological fluids. This protein has been deeply studied in the past few years because of its potential use as a strategy of drug targeting to tumor tissues. Chromium complex,  $[\text{Cr}(\text{phen})_3]^{3+}$  (phen = 1,10-phenanthroline), has been proposed as photosensitizers for photodynamic therapy (PDT). Thus, we analyzed the binding of chromium complex,  $[\text{Cr}(\text{phen})_3]^{3+}$ , to transferrin for a potential delivery of this diimine complex to tumor cells for PDT.

**Methods:** The interaction between  $[\text{Cr}(\text{phen})_3]^{3+}$  and holotransferrin (holoTf) was studied by fluorescence quenching technique, circular dichroism (CD) and ultraviolet (UV)–visible spectroscopy.

**Results:**  $[\text{Cr}(\text{phen})_3]^{3+}$  binds strongly to holoTf with a binding constant around  $10^9 \text{ M}^{-1}$ , that depends on the pH. The thermodynamic parameters indicated that hydrophobic interactions played a major role in the binding processes. The CD studies showed that there are no conformational changes in the secondary and tertiary structures of the protein.

**Conclusions:** These results suggest that the binding process would occur in a site different from the specific iron binding sites of the protein and would be the same in both protein states. As secondary and tertiary structures of transferrin do not show remarkable changes, we propose that the TfR could recognize the holoTf despite having a chromium complex associated.

**General significance:** Understanding the interaction between  $[\text{Cr}(\text{phen})_3]^{3+}$  with transferrin is relevant because this protein could be a delivery agent of Cr(III) complex to tumor cells. This can allow us to understand further the role of Cr(III) complex as sensitizer in PDT.

© 2014 Elsevier B.V. All rights reserved.

## 1. Introduction

Proteins are important macromolecules in our lives and main targets for drugs in the organism. Transferrin (Tf) is one of the most abundant serum proteins and it is responsible for the transport of both endogenous and exogenous compounds. In this regard, Tf is an important protein associated to the process of storage, transport and homeostasis of iron in vertebrates [1].

Transferrin is a monomeric 80-kDa glycoprotein, with a single polypeptide chain of about 679 amino acid residues, and two iron binding sites. Tf can be divided into two homologous regions: the N-terminal domain (residues 1 to 336) and the C-terminal domain (residues 337

to 679); each lobe consists of two domains (N<sub>1</sub> and N<sub>2</sub>, and C<sub>1</sub> and C<sub>2</sub>) that are connected by a flexible hinge. Each region shows a deep cleft capable of binding a metal ion. Each lobe of Tf binds one Fe<sup>3+</sup> ion tightly ( $\sim 10^{22} \text{ M}^{-1}$ ), yet reversibly. In both Tf lobes the Fe<sup>3+</sup> is coordinated by identical ligands: two tyrosine residues, one aspartic acid and one histidine residue (Tyr95, Tyr188, Asp63 and His249 in the N-lobe; Tyr426, Tyr517, Asp392 and His585 in the C-lobe). The distorted octahedral coordination of the iron is completed by a synergistic anion, identified as carbonate, which is anchored in place by a conserved arginine residue (Arg124 in the N-lobe and Arg456 in the C-lobe). When the binding sites are empty, the protein is known as apotransferrin (apoTf), the opposite occurs in the holotransferrin (holoTf) in which the sites are occupied. One of the major factors governing the binding and release of iron in transferrin is the pH [2–5]. In addition, it is also well-known that Tf is capable of binding to other cations such as Ti<sup>4+</sup>, Bi<sup>3+</sup>, Cr<sup>3+</sup> and Ru<sup>3+</sup>, besides Fe<sup>3+</sup> [6–8].

Tf undergoes a significant conformational change when binding and releasing iron. The binding of iron induces a rotation of the domains of approximately 60° producing a closed structure. The apoprotein possesses a more open conformation. This structural shift is very important in the

**Abbreviations:** Phen, 1,10-phenanthroline; HTf, human serum transferrin; apoTf, apotransferrin; holoTf, holotransferrin; TfR, transferrin receptor; PDT, photodynamic therapy; CD, circular dichroism; FRET, Förster resonance energy transfer

\* Corresponding author at: Instituto de Investigaciones en Físico Química de Córdoba – CONICET-UNC, Departamento de Físico Química, Facultad de Ciencias Químicas, Universidad Nacional de Córdoba, Ciudad Universitaria, X5000HUA Córdoba, Argentina. Tel.: + 54 351 4334169/80; fax: + 54 351 4334188.

E-mail address: [gerardo@fqc.unc.edu.ar](mailto:gerardo@fqc.unc.edu.ar) (G.A. Argüello).

iron metabolism, because the transferrin receptor (TfR), located in the cell membrane, is capable of recognizing only the rotated conformation [9]. Therefore, mainly holoTf can penetrate the cell and be incorporated by it, possibly by a mechanism that involves the formation of an endosome [10]. Once the endosome is internalized, its pH decreases from 7.40 (extracellular pH) to 5.60 by a proton pump, acidification that results in the release of the  $\text{Fe}^{3+}$ , and subsequent fusion of the endosome with the cell membrane to release and recycle the apoTf. [10–12].

On the other hand, chromium complexes have been suggested as possible photosensitizers for photodynamic therapy (PDT). We have demonstrated the capability of chromium(III) tris-diimine complexes,  $[\text{Cr}(\text{NN})_3]^{3+}$ , to induce DNA damage only by the excited state after irradiation with 452 nm light. In addition, these complexes also have the capability of impairing the survival of irradiated bacteria. The great advantage of these complexes is that they may not need oxygen to generate cell damage (Foot mechanism Type I) [13], making them good candidates to target hypoxic tumors [14,15].

Furthermore, tumor cells show evidence of a large demand of iron for their growth, therefore they have an overexpression of the TfR. As a matter of fact, in the last years, transferrin has been deeply studied because of its potential use as a strategy of drug targeting to tumor tissues [16–20]. This implies that the transferrin–drug system needs to preserve a proper affinity for the transferrin receptor so as to facilitate its interaction. It has been shown that transferrin promotes uptake of Ru(III) complexes into tumor cells [21]. Therefore, these properties of Tf have motivated us to investigate its interaction with polypyridyl Cr(III) complexes in order to evaluate whether this protein could act as a potential carrier of Cr(III) complexes to tumor cells.

Previously, we demonstrated the binding properties of  $[\text{Cr}(\text{phen})_2(\text{dppz})]^{3+}$  and  $[\text{Cr}(\text{phen})_3]^{3+}$  complexes with apoTf [22]. The results clearly indicated that  $[\text{Cr}(\text{phen})_2(\text{dppz})]^{3+}$  and  $[\text{Cr}(\text{phen})_3]^{3+}$  bind efficiently to apoTf. The values of association constants of the systems studied are of the same order of magnitude ( $10^5 \text{ M}^{-1}$ ), showing that the effect of the charge (+3) is not negligible and that the slight difference in the value of the constant could be attributed to the nature of the ligands. In addition, and in agreement with the results found in the fluorescence study, CD results indicate that although  $[\text{Cr}(\text{phen})_2(\text{dppz})]^{3+}$  and  $[\text{Cr}(\text{phen})_3]^{3+}$  could bind to the protein, no conformation change was observed. Due to the fact that the transferrin receptor, located in the cell membrane, is capable of recognizing only holoTf, it prompted us to study the binding properties of the Cr(III) complex to holoTf.

In the present work, we report a detailed study of the interaction of holoTf with  $[\text{Cr}(\text{phen})_3]^{3+}$ . The binding properties of the complex Cr(III)–holoTf were assessed by the use of the different spectroscopic techniques. In addition, we analyzed possible conformational changes in the holoTf– $[\text{Cr}(\text{phen})_3]^{3+}$  and apoTf– $[\text{Cr}(\text{phen})_3]^{3+}$  at different pHs, in order to get critical information for the potential use of Tf as a carrier of Cr(III) complex, and thus shed light on the applications of such molecules for photodynamic therapy.

## 2. Materials and methods

### 2.1. Materials

The chromium complex was synthesized as previously reported [23–25]. The stock solutions were prepared in a phosphate buffer solution (0.01 M  $\text{NaH}_2\text{PO}_4$ , 0.1 M NaCl, pH  $7.40 \pm 0.01$ ) and the concentrations of the complex's solutions were calculated using molar absorptivity values of  $4200 \text{ M}^{-1} \text{ cm}^{-1}$  at 354 nm. Bovine serum apotransferrin (essentially iron free bovine: minimum 98%, cell culture tested T1428) and bovine serum holotransferrin (holo-transferrin bovine  $\geq 95\%$ , Cell Culture Tested T1283) were purchased from Sigma Chemical Co., and used without further purification. For fluorescence studies, stock solutions of proteins were prepared in buffer solution and the concentrations were calculated using molar absorptivity values of  $74,400 \text{ M}^{-1} \text{ cm}^{-1}$  at 280 nm for apoTf and  $93,000 \text{ M}^{-1} \text{ cm}^{-1}$  at

280 nm for holoTf [26]. The solutions of complex and proteins for fluorescence studies were calibrated with HCl at three different pHs ( $7.40 \pm 0.01$ ;  $6.40 \pm 0.01$  and  $5.40 \pm 0.01$ ).

The stock solutions used to study secondary structure by circular dichroism (CD) were prepared in phosphate buffer (0.01 M  $\text{NaH}_2\text{PO}_4$ , 0.1 M  $\text{Na}_2\text{SO}_4$ ) at three different pHs ( $7.40 \pm 0.01$ ;  $6.40 \pm 0.01$  and  $5.40 \pm 0.01$ ) using  $\text{H}_2\text{SO}_4$  to calibrate the pH. According to S.M. Kelly et al., for the CD studies it is better to use anions such as sulfate or fluoride, which do not significantly absorb in this spectral range [27,28].

Millipore Milli Q water was used for preparing buffer solutions. All other chemical reagents were of analytical grade.

### 2.2. Spectroscopic measurements

The UV–visible spectra were recorded on an Agilent 8453 diode array detector spectrophotometer equipped with 1.0 cm quartz cells. Emission spectra were recorded at several temperatures on a Quanta Master QM2 spectrofluorometer from Photon Technology International equipped with a Hamamatsu R928 PMT in a photon counting detector using 1.0 cm quartz cells and thermostat bath, the excitation wavelengths were 280 and 295 nm, the excitation and emission slit widths were set at 5.0 nm. Appropriate blanks corresponding to the buffer were subtracted to correct background fluorescence. The CD spectra were recorded on a JASCO J-810 spectropolarimeter. Measurements were carried out in quartz cells of 1.0 cm path length. CD data were expressed as the mean residue ellipticity ( $[\theta]$ ).

### 2.3. Fluorescence measurements

The quenching effects of  $[\text{Cr}(\text{phen})_3]^{3+}$  on holoTf at different pHs and temperatures were shown by the well-known Stern–Volmer equation (Eq. (1)) [29]

$$F_0/F = 1 + k_q\tau_0[Q] = 1 + K_{sv}[Q] \quad (1)$$

where  $F_0$  and  $F$  are the fluorescence intensities in the absence and the presence of quencher respectively;  $[Q]$  is the concentration of quencher (Cr(III) complex);  $k_q$  is the biomolecular quenching rate constant and  $\tau_0$  is the average lifetime of the fluorophore in the absence of quencher with a value of  $10^{-8} \text{ s}$  [30]; and  $K_{sv}$  is the Stern–Volmer dynamic quenching constant.

The fluorescence intensities used in this study were all corrected for absorption of the exciting light and re-absorption of emitted light (internal filter) using Eq. (2) [31]:

$$F_{cor} = F_{obs} 10^{(-\epsilon_{exc}l_1c)} (1 - 10^{(-\epsilon_{exc}l_2c)}) \cdot 10^{(-\epsilon_{em}l_3c)} \quad (2)$$

where  $F_{cor}$  and  $F_{obs}$  are the fluorescence intensities corrected and observed, respectively,  $\epsilon_{exc}$  and  $\epsilon_{em}$  are the extinction coefficients of the system at excitation and emission wavelengths, respectively, and  $l_1$ ,  $l_2$  and  $l_3$  are parameters that take into account the travel distance of the beam in the quartz cell, 0.4, 0.2 and 0.5 cm, respectively.

### 2.4. Binding assays

The binding constants were determined by fluorescence intensity of holoTf with  $[\text{Cr}(\text{phen})_3]^{3+}$ . First, the emission spectrum of protein was recorded at a concentration of  $1.5 \times 10^{-6} \text{ M}$ , using a volume of 1.5 ml and subsequently, the spectra of the same solution of the protein were recorded in the presence of increasing concentrations of Cr(III) complex, ranging from 0 up to  $10 \times 10^{-6} \text{ M}$ . The intrinsic binding constants were determined from the decrease of the intensity at 327 nm ( $\lambda_{max}$ ), with increasing concentrations of Cr(III) complex according to the Bhattacharyya model (Eq. (3)) [32,33]:

$$1/\Delta F = 1/\Delta F_{max} + (1/\Delta F_{max} K_b) \times (1/[Q]), \quad (3)$$

where  $\Delta F = F_\lambda - F_0$  and  $\Delta F_{\max.} = F_\infty - F_0$ , where  $F_0$ ,  $F_\lambda$  and  $F_\infty$  are the fluorescence intensities of protein in the absence of Cr(III) complex, at an intermediate concentration of Cr(III) complex and at the saturation of interaction, respectively;  $K_b$  being the binding constant and  $[Q]$  the Cr(III) complex concentration. The linearity in the plot of  $1/\Delta F$  against  $1/[Q]$  confirms a one-to-one interaction between the two components. The binding constants were determined at several temperatures to calculate the thermodynamic parameters for the association processes.

### 2.5. Forster resonance energy transfer

In this work, the efficiency of energy transfer was studied according to Förster's non-radiative energy transfer theory where the efficiency of energy transfer,  $E$ , is described by Eq. (4) [34,35]:

$$E = 1 - F/F_0 = R_0^6 / (R_0^6 + r^6) \quad (4)$$

where  $F_0$  and  $F$  are the fluorescence intensities of holoTf (donor) in the absence and the presence of Cr(III) complex (acceptor),  $r$  is the distance between acceptor and donor, and  $R_0$  is the critical distance when the transfer efficiency is 50%.  $R_0$  is determined from Eq. (5):

$$R_0^6 = 8.8 \times 10^{-25} \kappa^2 \eta^{-4} \Phi J \quad (5)$$

here,  $\kappa^2$  is the spatial orientation factor describing the relative orientation in the space of the transition dipoles of the donor and acceptor,  $\eta$  is the refractive index of the medium,  $\Phi$  is the fluorescence quantum yield of the donor in the absence of the acceptor, and  $J$  is the overlap integral of the fluorescence emission spectrum of the donor and the absorption spectrum of the acceptor.  $J$  is given by Eq. (6):

$$J = \left[ \frac{\sum F(\lambda) \varepsilon(\lambda) \lambda^4 \Delta\lambda}{\sum F(\lambda) \Delta\lambda} \right] \quad (6)$$

where  $F(\lambda)$  is the fluorescence intensity of the donor at wavelength  $\lambda$ , and  $\varepsilon(\lambda)$  is the molar absorption coefficient of the acceptor at wavelength  $\lambda$  when both spectra are recorded at the same concentration. In this case,  $\kappa^2 = 2/3$ ,  $\eta = 1.33$  and  $\Phi = 0.13$  [35,36].

From the above relationships,  $J$  and  $E$  can be easily obtained; therefore,  $R_0$  and  $r$  can be further calculated for a molar ratio Cr(III) complex:protein 1:1.

### 2.6. Circular dichroism

CD spectra of apoTf and holoTf ( $c_{\text{protein}} = 4.8 \times 10^{-7}$  M) and the apoTf–Cr(III) complex at a molar ratio ( $r_i$ ) of Cr(III) to protein of  $r_i = 2.0$  were recorded in the wavelength region 200 to 250 nm at different pHs. The corresponding absorbance contributions of buffer and free Cr(III) complex solutions were recorded and subtracted with the same instrumental parameters. The CD results were expressed in terms of mean residue ellipticity ( $[\theta]$ ) in  $^\circ \text{cm}^2 \text{dmol}^{-1}$  according to Eq. (7):

$$[\theta] = \text{observed CD (mdeg)} / (10 \cdot C_p \cdot n \cdot l) \quad (7)$$

where  $C_p$  is the molar concentration of the protein ( $\text{mol} \cdot \text{cm}^{-3}$ ),  $n$  is the number of amino acid residues, and  $l$  is the path length (cm) [37].

## 3. Results and discussion

### 3.1. Quenching experiment

As it is shown in Fig. 1, when a fixed concentration of protein was titrated with different concentrations of  $[\text{Cr}(\text{phen})_3]^{3+}$  complex, the fluorescence intensity of the holoTf decreases, while the emission maximum remained unchanged. This indicates that the complex binds to

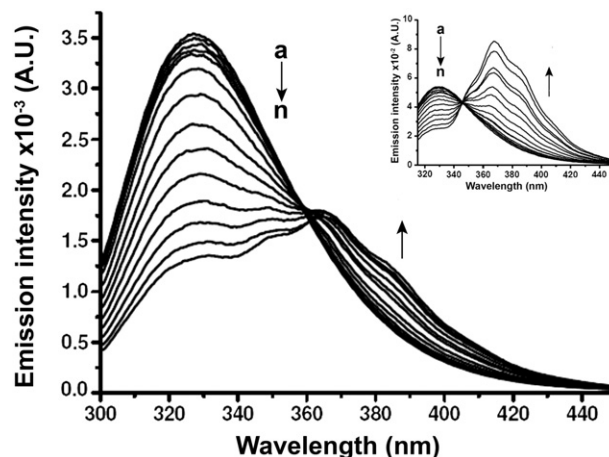


**Fig. 1.** Fluorescence emission spectra of holoTf in the absence or presence of  $[\text{Cr}(\text{phen})_3]^{3+}$ . The concentration of protein was fixed at  $1.5 \times 10^{-6}$  M; the concentrations of Cr(III) complexes from a to n were (0, 0.14, 0.29, 0.44, 0.59, 0.87, 1.1, 1.6, 2.5, 3.4, 4.6, 5.8, 7.1 and  $8.4) \times 10^{-6}$  M, respectively; T = 298 K, pH 7.4;  $\lambda_{\text{exc}} = 280$  nm,  $\lambda_{\text{em}} = 327$  nm. Inset same spectra at  $\lambda_{\text{exc}} = 295$  nm. Both excitation and emission slits were 5 nm.

holoTf without altering the environment surrounding the chromophore residues. The emission spectrum from the quencher does not overlap with the emission spectra of the protein at the wavelengths of measurement  $\lambda_{\text{em}} = 327$  nm. Similar behaviors were found for Toneatto et al. in previous works [22,33].

The decrease in fluorescence intensity resulted from the reduction of the fluorescence quantum yield, as a consequence of a decrease in the electronic density once the Cr(III) complex molecule entered a hydrophobic cavity of holoTf. The quenching took place when the quencher was sufficiently close to the tryptophanyl and tyrosyl residues. ApoTf and holoTf have 8 tryptophan residues and 26 tyrosine residues, located in both lobes of the protein [38]. When excitation wavelength of  $\lambda = 280$  nm is used, fluorescence of protein arises from both tyrosine and tryptophan. However, when wavelength of  $\lambda = 295$  nm is used, only the tryptophan moiety is excited. Consequently, to determine whether both residues are involved in the deactivation of the fluorescence of the protein, we compared the emission exciting the sample at 280 nm and 295 nm in the presence of different complex concentrations. When the molar ratio ( $r_i$ ) of complex to protein was  $r_i = 3.7$ , the fluorescence of holoTf excited at 280 nm and 295 nm decreased by 64% and 51%, respectively (Fig. 2A). This remarkable difference shows that both amino acids are involved in the quenching process.

The different mechanisms of quenching are usually classified either as static or dynamic quenching. The former refers to the formation of a non-fluorescent fluorophore–quencher complex. In contrast, dynamic quenching refers to the diffusion of the quencher to the fluorophore during the lifetime of the excited state, and upon contact, the fluorophore returns to ground state without emission of a photon [39]. A probable quenching mechanism for holoTf and Cr(III) complex is evidenced from the Stern–Volmer plot (Fig. 2B). A positive curvature in the Stern–Volmer plot (Eq. (1)) can be observed. This result indicates that both mechanisms (static and dynamic) of quenching can take place in the protein association process. This behavior has been described in processes of binding between Cr(III) complexes with apoTf and albumins [22,33]. This type of deviation occurs when quencher molecules interact with tryptophan and tyrosine residues causing the fluorescence quenching; then they change their position within the fluorophore microenvironment making room for the other molecules of the quencher. Further, it has been recently demonstrated in similar systems that the contribution of dynamic quenching seems to be less than the static quenching [21].

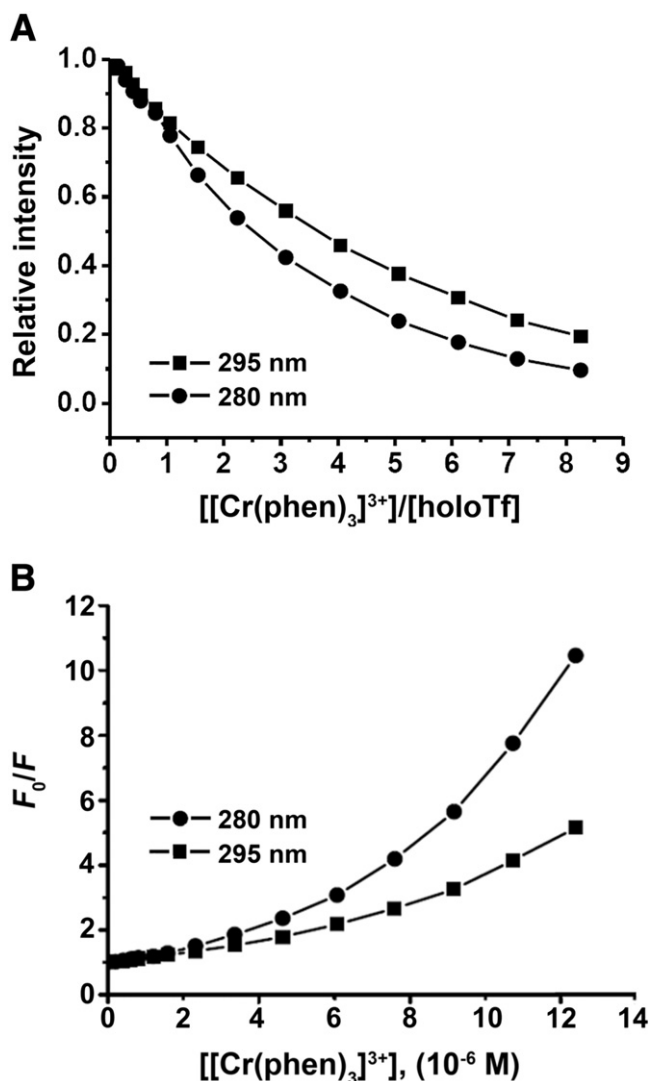


Fig. 2. A – Relative fluorescence intensity and B – Stern–Volmer plots at  $\lambda_{em} = 327$  nm upon titration of holoTf with increasing amounts of  $[\text{Cr}(\text{phen})_3]^{3+}$  at two different excitation wavelengths  $\lambda_{ex} = 280$  nm (●) and 295 nm (■).  $T = 298$  K; pH 7.40.

### 3.2. Association between the complex and the transferrin. Effect of the pH

In order to further characterize the interaction between  $[\text{Cr}(\text{phen})_3]^{3+}$  and holoTf, the binding constant,  $K_b$ , was determined at different pHs and temperatures, from the fluorescence intensity data using Eq. (3). Table 1 shows the binding parameters obtained from the interaction of  $[\text{Cr}(\text{phen})_3]^{3+}$  with holoTf and apoTf at different pHs. It was found that the binding constants diminished with the decrease of pH ranging from extracellular pH (approximately 7.40) to endosomal pH (approximately 5.40) for both systems (Fig. 3).

Table 1

Binding parameters obtained from the interaction of  $[\text{Cr}(\text{phen})_3]^{3+}$  with apoTf and holoTf at different pHs.

pH	apoTf– $[\text{Cr}(\text{phen})_3]^{3+}$		holoTf– $[\text{Cr}(\text{phen})_3]^{3+}$	
	$K_b$ ( $\times 10^5 \text{ M}^{-1}$ )	$r$	$K_b$ ( $\times 10^5 \text{ M}^{-1}$ )	$r$
$7.40 \pm 0.01$	$1.5 \pm 0.2$	0.9997	$1.5 \pm 0.3$	0.9995
$6.40 \pm 0.01$	$1.0 \pm 0.2$	0.9997	$1.1 \pm 0.2$	0.9995
$5.40 \pm 0.01$	$0.7 \pm 0.1$	0.9995	$0.43 \pm 0.07$	0.9997

The parameters were calculated from the data in Fig. 1 using Eq. (3);  $r$  is the regression coefficient.

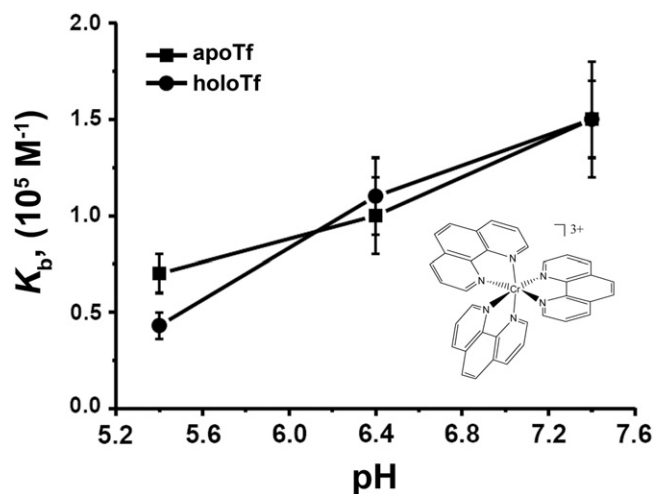


Fig. 3. Plot of binding constant ( $K_b$ ) vs. pH for holoTf– $[\text{Cr}(\text{phen})_3]^{3+}$  system (●) and apoTf– $[\text{Cr}(\text{phen})_3]^{3+}$  system (■);  $T = 298$  K. Inset, molecular graph of  $[\text{Cr}(\text{phen})_3]^{3+}$ .

All measured binding constants are approximately in the order of  $10^5 \text{ M}^{-1}$ ; these are higher constants compared with ruthenium complexes which are in the order of  $10^3 \text{ M}^{-1}$ – $10^4 \text{ M}^{-1}$  [21,40,41].

A variety of amino acid residues as well as the carboxyl and amide termini of proteins have a pKa range in the same range as intracellular pH. As a result, a change in pH can protonate or deprotonate a side group, thereby changing its chemical features. At low pH, protonation of an acid residue might be favored generating more repulsion with the chromium complex (+3) and making the association more difficult. According to the pKas of aminoacids, histidine (pKa = 6.04, in the imidazole group) could be protonated, indicating that this amino acid should be presently close to the binding site.

Interestingly, the binding constant values for both systems studied are similar (Table 1 and Fig. 3), suggesting that the binding process could occur in a site different from the specific iron binding sites of the protein and that the Cr(III) complex association site could be the same in both protein states (apo and holo). If the complex binds to the apoTf at the iron site, its constant should be very different to the binding constant of holoTf–Cr(III) complex due to the electrostatic repulsion of the iron cation in the cavity. Moreover, the iron cation cannot be substituted by the chromium complex due to the high binding constant of iron for transferrin ( $\sim 10^{22} \text{ M}^{-1}$ ).

Table 2 shows the binding constants obtained from the interaction of  $[\text{Cr}(\text{phen})_3]^{3+}$  with holoTf at different temperatures. It was found that the binding constants increase when the temperature rises, resulting in an enhancement in the stability of protein–Cr(III) association.

### 3.3. Binding mode

Generally, small molecules are bound to macromolecules mainly through four binding modes: hydrogen bond, van der Waals force, and

Table 2

Binding parameters obtained from the interaction of Cr(III) complex with holoTf at pH = 7.40.

T (K)	holoTf– $[\text{Cr}(\text{phen})_3]^{3+}$	
	$K_b$ ( $\times 10^5 \text{ M}^{-1}$ )	$r$
298	$1.0 \pm 0.1$	0.999
302	$2.4 \pm 0.3$	0.997
305	$3.5 \pm 0.8$	0.992

The parameters were calculated from the data in Fig. 1 using Eq. (3);  $r$  is the regression coefficient.



electrostatic and hydrophobic interactions [42]. The thermodynamic parameters, enthalpy ( $\Delta H$ ) and entropy ( $\Delta S$ ) of the reaction, are important to determine the acting force. For this reason, the temperature dependence of the binding constant was studied. If we assume that the  $\Delta H$  does not vary significantly over the temperature range studied, then, its value as well as the one for  $\Delta S$  can be determined from the Vant's Hoff's equation by plotting the values of  $\ln K_b$  vs.  $1/T$ . The temperatures used were 298, 302 and 305 K and the enthalpy and entropy changes ( $\Delta H$  and  $\Delta S$ ) were calculated from the slope and ordinate of the Vant's Hoff relationship. The free energy change ( $\Delta G$ ) is estimated from the following relationship  $\Delta G = \Delta H - T \cdot \Delta S$  by fitting the data of Fig. 4. Table 3 summarizes the values of  $\Delta G$ ,  $\Delta H$  and  $\Delta S$  obtained for the binding site.

Many references have reported the characteristic sign of the thermodynamic parameter associated with the various individual kinds of interaction that may take place in the protein association process [43,44]. From the point of view of water structure for ligand–protein interaction, the positive values of entropy and enthalpy are frequently offered as evidence for the hydrophobic interaction, because the presence of a ligand in the protein makes the water molecules acquire a more random structure around the site of association. The negative values of  $\Delta G$  seen in Table 3 support the assertion that the binding process is spontaneous. The positive  $\Delta S$  and  $\Delta H$  values of the interaction of Cr(III) complex and holoTf indicate that the binding is mainly an entropy-driven process and the enthalpy is unfavorable for it, suggesting that a hydrophobic interaction may play a major role in the reaction. This is expected to play a role since the ligands of the complex are rather hydrophobic. However, the electrostatic interaction cannot be excluded in view of the charges of the species involved. These results reveal that the  $[\text{Cr}(\text{phen})_3]^{3+}$  stabilizes holoTf with a strong entropic contribution as was found for the process of binding between  $[\text{Cr}(\text{phen})_3]^{3+}$  and apoTf [22] and  $[\text{Cr}(\text{phen})_3]^{3+}$  and albumin [33].

#### 3.4. Energy transfer from holotransferrin to $[\text{Cr}(\text{phen})_3]^{3+}$

Förster resonance energy transfer (FRET) is a non-destructive spectroscopic method that can monitor the proximity and relative angular orientation of fluorophores and the acceptor. The donor and acceptor can be entirely separate or attached to the same macromolecule. A transfer of energy could take place through direct electrodynamic interaction between the primarily excited molecule and its neighbors [45]. The spectroscopic ruler is suitable for distance measurement over several nanometers [46]. Using FRET, the distance  $r$  of binding between Cr(III) complex and holoTf could be calculated by the Eq. (4).

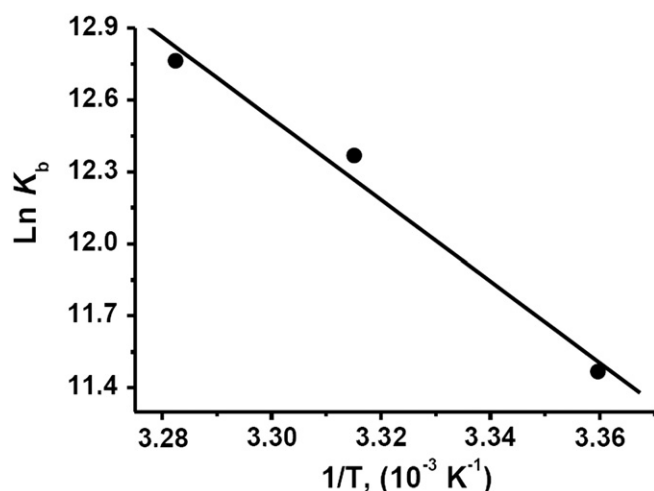


Fig. 4. Van't Hoff plot ( $\ln K_b$  vs.  $1/T$ ) for holoTf– $[\text{Cr}(\text{phen})_3]^{3+}$  system.

**Table 3**  
Thermodynamic parameters of the holoTf– $[\text{Cr}(\text{phen})_3]^{3+}$  system.

T (K)	$\Delta G$ ( $\text{kJ mol}^{-1}$ )	$\Delta H$ ( $\text{kJ mol}^{-1}$ )	$\Delta S$ ( $\text{J mol}^{-1} \text{ K}^{-1}$ )
298	$-30 \pm 7$		
302	$-32 \pm 8$	$140 \pm 2$	$570 \pm 6$
305	$-34 \pm 8$		

Data were calculated with Van't Hoff's equation; the regression coefficients were  $r = 0.99124$ .

Generally, FRET occurs whenever the emission spectrum of a fluorophore (donor) overlaps the absorbance spectrum of another molecule (acceptor). The overlap of the UV absorption spectra of  $[\text{Cr}(\text{phen})_3]^{3+}$  (acceptor) with the fluorescence emission spectrum of holoTf (donor) ( $\lambda_{\text{exc.}} = 280 \text{ nm}$ , pH 7.40) is shown in Fig. 5. Similar results were obtained at pH 6.40 and 5.40 (data not shown).

The overlap integral  $J$  could be evaluated by investigating the spectra seen in Fig. 5. By Eq. (5), the critical distance  $R_0$  could be calculated for the binding process. Table 4 shows the parameters regarding the FRET. Each value of  $r$  was less than  $2R_0$  and ranged in the efficient distance (2–7 nm) for FRET, which indicated a reliability of the results and the occurrence of FRET between holoTf and the Cr(III) complex. Moreover, the results in Table 4 suggested that the bound  $[\text{Cr}(\text{phen})_3]^{3+}$  had an equal distance to the Trp at all pHs tested. One explanation for this result is that the kind of binding sites for Cr(III) complex in holoTf did not change at the pHs tested.

The average distances between a donor fluorophore and acceptor fluorophore on the 2–8 nm scale [47] and  $0.5R_0 < r < 1.5R_0$  [36], which indicate that the energy transfer from holoTf to  $[\text{Cr}(\text{phen})_3]^{3+}$  occurs with high probability. This was in agreement with the conditions of the Förster non-radiative resonance energy transfer theory and again being the consequence of a quenching between Cr(III) complex and holoTf.

#### 3.5. Structural changes induced by $[\text{Cr}(\text{phen})_3]^{3+}$

When molecules bind to proteins, they can produce conformational changes in the protein, altering the secondary and/or tertiary structure. In the case of Tf, its membrane receptor has a very high affinity for the holoTf instead of the apoTf [1]. Between these two states of the protein there is a huge conformational change in the tertiary structure that

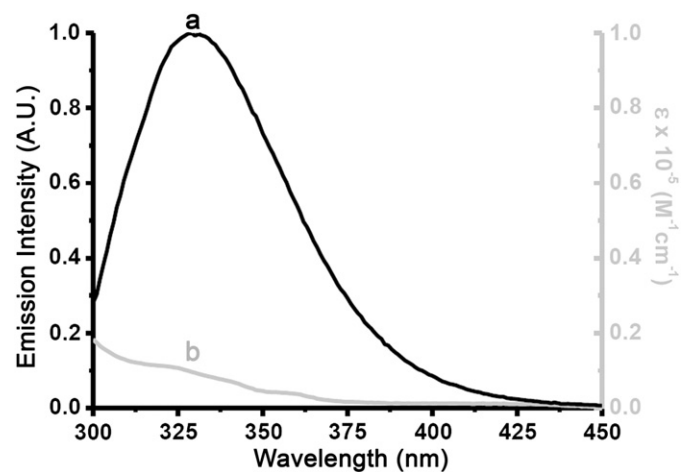


Fig. 5. The fluorescence emission spectrum of holoTf ( $\lambda_{\text{exc.}} = 280 \text{ nm}$ ) (a) overlaps with the absorption spectra of  $[\text{Cr}(\text{phen})_3]^{3+}$  (b). The concentrations of Cr(III) complex and protein were  $1.5 \times 10^{-6} \text{ M}$ ;  $T = 298 \text{ K}$ .

**Table 4**

Parameters regarding the Förster's non-radiative energy transfer theory for the holoTf-[Cr(phen)<sub>3</sub>]<sup>3+</sup> system at different pHs.

Parameters	pH = 7.40 ± 0.01	pH = 6.40 ± 0.01	pH = 5.40 ± 0.01
<i>J</i>	8.93 × 10 <sup>-15</sup> cm <sup>3</sup> l mol <sup>-1</sup>	8.94 × 10 <sup>-15</sup> cm <sup>3</sup> l mol <sup>-1</sup>	9.28 × 10 <sup>-15</sup> cm <sup>3</sup> l mol <sup>-1</sup>
<i>E</i>	0.227	0.235	0.216
<i>r</i>	3.01 nm	2.99 nm	3.06 nm
<i>R</i> <sub>0</sub>	2.45 nm	2.45 nm	2.47 nm

Data were calculated according to Eqs. (4) to (6); *J* is the overlap integral of the fluorescence emission spectrum of the donor and the absorption spectrum of the acceptor, *E* is the efficiency of energy transfer, *r* is the distance between acceptor and donor, and *R*<sub>0</sub> is the critical distance when the transfer efficiency is 50%.

corresponds to a series of rotations of the lobes and domains of the protein [48]. These rotations promote a remarkable change in the tertiary structure spectra.

In order to determine if the binding of the complex with the protein induces conformational changes, we used circular dichroism to study secondary and tertiary structures at different concentrations of complex and at different pHs.

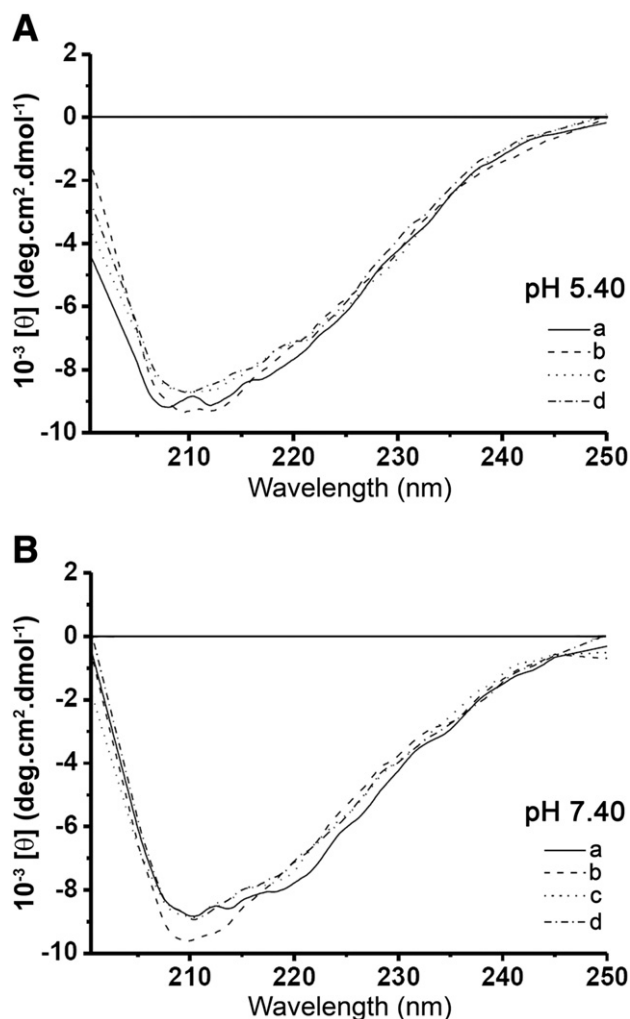


**Fig. 6.** Circular dichroism spectra from 200 nm to 250 nm of holoTf in the presence or the absence of [Cr(phen)<sub>3</sub>]<sup>3+</sup> (A) at pH 5.40 and (B) at pH 7.40. The concentration of protein was fixed at 1.5 × 10<sup>-6</sup> M; the molar ratios of [Cr(phen)<sub>3</sub>]<sup>3+</sup>/protein from a to d were 0, 0.5, 1.0, and 2.0, respectively; T = 298 K, 0.04 M phosphate and 0.1 M of sulfate.

For the analysis of the secondary structure we study the region between 200 nm and 250 nm using a protein concentration of 1.5 × 10<sup>-6</sup> M and different concentrations of chromium complex. The experiments were performed at pH 5.40, 6.40 and 7.40 (pH ± 0.01) for both holoTf and apoTf, so we can evaluate the behavior of the binding between [Cr(phen)<sub>3</sub>]<sup>3+</sup> with the protein at endosomal and extracellular pHs.

As can be observed in Fig. 6, the CD spectrum of holoTf (spectrum a) exhibits two negative bands in the ultraviolet region at 208 and 218 nm approximately, characteristic of an α-helical structure of protein. When [Cr(phen)<sub>3</sub>]<sup>3+</sup> was added to the solution of holoTf (spectra b to d) no significant changes were observed in the spectra, even at different pHs. The same behavior was found for the apoTf (data not shown). Thus, the complex does not produce considerable conformational changes in the protein.

In order to study the tertiary structure, we analyzed the CD spectra in the visible region (320–500 nm) using a protein concentration of 1 × 10<sup>-4</sup> M and different concentrations of Cr(III) complex at pH 7.40.

Fig. 7 shows the typical CD spectrum of holoTf (spectrum a) characterized by two bands, a minimum and a maximum at 450 and 334 nm, respectively, and weak signals which are attributed to the presence of aromatic residues (phenylalanine at 255–270 nm, tyrosine at 280 nm and tryptophan at 290 nm) in the region between 250 and 300 nm. When [Cr(phen)<sub>3</sub>]<sup>3+</sup> was added to the solution of holoTf (spectra b and c) no significant changes were observed in the spectra of the protein, indicating that the presence of the complex does not produce significant conformational changes in the protein. ApoTf has been studied in a previous work and showed no changes at all in the tertiary structure [22].

Taken together these results demonstrate that [Cr(phen)<sub>3</sub>]<sup>3+</sup> can bind to holoTf and apoTf, without altering the secondary or tertiary structure of the proteins. These observations are consistent with the results obtained in the fluorescence and thermodynamic experiments, from which it was concluded that the binding could occur in a site different from the specific iron binding sites of Tf. It is possible that the binding of the Cr(III) complex may take place in hydrophobic patches present in Tf near iron binding site. Furthermore, Trp and Tyr residues may be involved, among others, as we have recently demonstrated for the [Cr(phen)<sub>3</sub>]<sup>3+</sup>-apoTf association complex [22].

The fact that secondary and tertiary structures do not have remarkable structural changes leads us to think that the TfR would recognize the holoTf despite having a chromium complex associated.

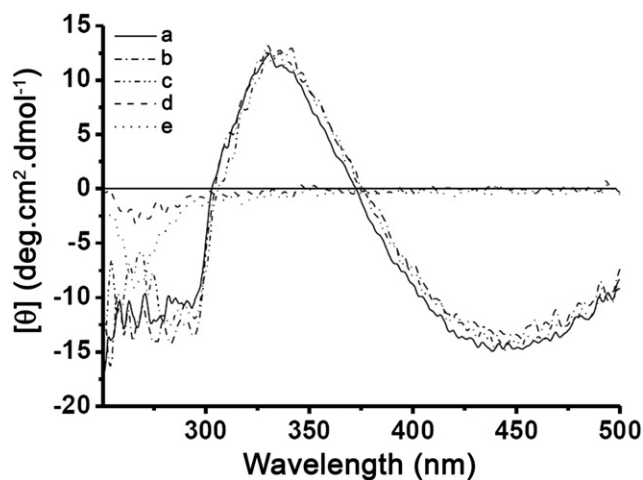


**Fig. 7.** Circular dichroism spectra from 250 nm to 500 nm of holoTf in the absence or the presence of [Cr(phen)<sub>3</sub>]<sup>3+</sup>. Protein concentration was fixed at 1 × 10<sup>-4</sup> M, and from a to c the molar ratios of [Cr(phen)<sub>3</sub>]<sup>3+</sup>/protein were 0, 5 and 10 respectively; d and e were circular dichroism spectra from [Cr(phen)<sub>3</sub>]<sup>3+</sup> at 1 × 10<sup>-6</sup> and 2.2 × 10<sup>-6</sup> M, respectively.

#### 4. Conclusions

The present study describes and explains the nature and magnitude of the interactions between  $[\text{Cr}(\text{phen})_3]^{3+}$  and holotransferrin at different conditions of pH and temperature. The binding process has been investigated by fluorescence, UV absorption and CD spectroscopic approaches. We showed that  $[\text{Cr}(\text{phen})_3]^{3+}$  binds strongly with holotransferrin, with an intrinsic binding constant in the order of  $10^5 \text{ M}^{-1}$ . In addition, the binding constants increase when the temperature rises, resulting in an enhancement in the stability of protein–Cr(III) complex association and diminished with the pH decrease from extracellular to endosomal pH (approximately from 7.40 to 5.40). Interestingly, the binding constant values for  $[\text{Cr}(\text{phen})_3]^{3+}$ –holoTf and –apoTf systems studied are similar, suggesting that the binding process would occur in a site different from the specific iron binding sites of the protein and that the Cr(III) complex association site could be the same in both protein states (apo and holo). The fact that secondary and tertiary structures of the protein do not have remarkable changes leads us to think that the TfR would recognize the holoTf despite having a chromium complex associated. This is a relevant finding because holoTf is known as an important carrier to target tumor cells, and therefore our study poses a new venue in photodynamic therapy that needs to be further explored.

#### Acknowledgements

The author thanks Consejo Nacional de Investigaciones Científicas y Técnicas de Argentina (CONICET), Secretaría de Ciencia y Técnica de la Universidad Nacional de Córdoba (SeCyT-UNC) and Agencia Nacional de Promoción de la Ciencia y la Técnica (ANPCyT) for financial support (PIP 2011–2013 CONICET 11220100100480). P.F.G. and J.T. are research fellows from CONICET. M.J.S. is a research fellow from ANPCyT. G.A.A. is an Independent Researcher from CONICET.

#### References

- [1] H. Sun, H. Li, P.J. Sadler, *Chem. Rev.* 99 (1999) 2817–2842.
- [2] H.A. Heubers, C.A. Finch, *Physiol. Rev.* 67 (1987) 520–582.
- [3] J. Fletcher, E.R. Heuhns, *Nature* 215 (1967) 584–586.
- [4] R.C. Roberts, D.G. Makey, *J. Biol. Chem.* 241 (1966) 4907–4950.
- [5] K.G. Mann, W.W. Fish, A.C. Fish, C. Tanford, *Biochemistry* 9 (1970) 1348–1350.
- [6] A.L. Vavere, M.J. Welch, *J. Nucl. Med.* 46 (2005) 683–690.
- [7] M.J. Clarke, *Coord. Chem. Rev.* 236 (2003) 209–233.
- [8] J. Vincent, S. Love, *Biochim. Biophys. Acta* 1820 (2012) 362–378.
- [9] P. Aisen, in: A. Sigel, H. Sigel (Eds.), *Metal Ions in Biological Systems*, Marcel Dekker, New York, 1998, p. 585.
- [10] G. Perez, D. Vittori, N. Pregi, G. Garbossa, A. Nesse, *Acta Bioquím. Clín. Latinoam.* vol. 39 (no. 3) (2005) 301–314 (ISSN 1851–6114).
- [11] A. Steere, S. Byrne, N. Chasteen, A. Mason, *Review, Biochim. Biophys. Acta* 1820 (2012) 326–333.
- [12] N. James, S. Byrne, A. Mason, *Biochim. Biophys. Acta* 1794 (2009) 532–540.
- [13] C.S. Foote, *Science* 162 (1968) 963–970.
- [14] J. Toneatto, G. Lorenzatti, A.M. Cabanillas, G.A. Argüello, *Inorg. Chem. Commun.* 15 (2012) 43–46.
- [15] J. Toneatto, R.A. Boero, G. Lorenzatti, A.M. Cabanillas, G.A. Argüello, *J. Inorg. Biochem.* 104 (2010) 697–703.
- [16] L. Esserman, S. Takahashi, V. Rojas, R. Warnke, R. Levy, *Blood* 74 (1989) 2718–2729.
- [17] R. Sciot, A.C. Paterson, P. Van Eyken, F. Callea, M.C. Kew, V.J. Desmet, *Histopathology* 12 (1988) 53–63.
- [18] P.T. Gomme, K.B. MacCann, *Adv. Drug Deliv. Rev.* 10 (2005) 267–273.
- [19] H. Du, J. Xiang, Y. Zhang, Y. Tang, G. Xu, *J. Inorg. Biochem.* 102 (2008) 146–149.
- [20] A. Bergamo, G. Sava, *Dalton Trans.* 40 (2011) 7817–7823.
- [21] O. Mazuryk, K. Kurpiewska, K. Lewinski, G. Stochel, M. Brindell, *J. Inorg. Biochem.* 116 (2012) 11–18.
- [22] J. Toneatto, P.F. Garcia, G.A. Argüello, *J. Inorg. Biochem.* 105 (2011) 1299–1305.
- [23] K.D. Barker, K.A. Barnett, S.M. Connell, J.W. Glaeser, A.M. Wallace, J. Wildsmith, B.J. Herbert, J.F. Wheeler, N.A.P. Kane-Maguire, *Inorg. Chem. Acta* 316 (2001) 41–49.
- [24] N. Serpone, M.A. Jamieson, M.S. Henry, M.Z. Hoffman, F. Bolletta, M. Maestri, *J. Am. Chem. Soc.* 101 (1979) 2907–2916.
- [25] D. Pagliero, G.A. Argüello, E.H. Staricco, *J. Photochem. Photobiol. A Chem.* 115 (1998) 199–206.
- [26] D.M. Martin, N.D. Chasteen, J.K. Grady, *Biochim. Biophys. Acta* 1076 (1991) 252–258.
- [27] S. Kelly, N. Price, *Curr. Protein Pept. Sci.* 1 (2000) 349–384.
- [28] B.A. Wallace, *Q. Rev. Biophys.* 42 (2009) 317–370.
- [29] T.J. Dewey, *Biophysical and Biochemical Aspects of Fluorescence Spectroscopy*, Plenum, New York, 1991, 1–41.
- [30] J.R. Lakowicz, G. Weber, *Biochemistry* 12 (1973) 4161–4170.
- [31] S. Sarzeshi, J. Chamani, *Int. J. Biol. Macromol.* 47 (2010) 558–569.
- [32] J. Bhattacharyya, M. Bhattacharyya, A.S. Chakrabarty, U. Chaudhuri, R.K. Poddar, *Biochem. Pharmacol.* 47 (1994) 2049–2052.
- [33] J. Toneatto, G.A. Argüello, *J. Inorg. Biochem.* 105 (2011) 645–651.
- [34] T. Förster, O. Sinanoglu (Eds.), *Modern Quantum Chemistry*, vol. 3, Academic Press, New York, 1996, p. 93.
- [35] J.R. Lakowicz, *Principles of Fluorescence Spectroscopy*, 2nd ed. Kluwer/Plenum, New York, 1999, 237–265.
- [36] B. Valeur, *Molecular Fluorescence Principles and Applications*, Wiley-VCH, 2002, 247–254.
- [37] R.W. Woody, *Theory of circular dichroism of proteins*, in: G.D. Fasman (Ed.), *Circular Dichroism and the Conformational Analysis of Biomolecules*, Plenum Press, New York, USA, 1996, pp. 25–67.
- [38] R.T. MacGillivray, E. Mendez, J.G. Shewale, S.K. Sinha, J. Lineback-Zins, K. Brew, *J. Biol. Chem.* 258 (1983) 3543–3553.
- [39] F. Morero, M. Cortijo, J.G. Jimenez, *Photochem. Photobiol.* 70 (1999) 695–700.
- [40] Zahra Jannesari, Hassan Hadadzadeh, Taghi Khayamian, Batool Maleki, Hadi Amiri Rudbari, *Eur. J. Med. Chem.* 69 (2013) 577–590.
- [41] Eththilu Babua, Paulpandian Muthu Mareeswarana, Subramanian Singaravavel, Jayaraman Bhuvanewari, Seenivasan Rajagopal, *Spectrochim. Acta A Mol. Biomol. Spectrosc.* 130 (2014) 553–560.
- [42] S.N. Timaseff, *Proteins of Biological Fluids*, in: H. Peeters (Ed.), Pergamon Press, Oxford, 1972, pp. 511–519.
- [43] N. Juziro, M. Noriko, *Chem. Pharm. Bull.* 33 (1985) 2522–2524.
- [44] P.D. Ross, S. Subramanian, *Biochemistry* 20 (1981) 3096–3102.
- [45] T. Förster, *Ann. Phys.* 2 (1948) 55–75.
- [46] A.P. Silva, H.Q.N. Gunaratne, T. Gunnlaugsson, A.J.M. Huxley, C.P. McCoy, J.T. Rademacher, T.E. Rice, *Chem. Rev.* 97 (1997) 1515–1567.
- [47] S. Weiss, *Science* 283 (1999) 1676–1683.
- [48] Piyali Guha Thakurta, Debi Choudhury, Rakhi Dasgupta, J.K. Dattagupta, *Biochem. Biophys. Res. Commun.* 316 (2004) 1124–1131.